

# Static and seismic design of Dry Stone Retaining Walls (DSRWs) following Eurocode standards

**Nathanaël SAVALLE<sup>1,2a\*</sup>, Christine MONCHAL<sup>3b</sup>, Eric VINCENS<sup>4c</sup>, Sten FORCIOLI<sup>3d</sup> and Paulo B. LOURENÇO<sup>1e</sup>**

<sup>1</sup> University of Minho, ISEC, Department of Civil Engineering, Guimarães, Portugal

<sup>2</sup> Université Clermont Auvergne, Clermont Auvergne INP, CNRS, Institut Pascal, F-63000 Clermont–Ferrand, France

<sup>3</sup> Géolithe – Grenoble : 181 rue des Bécasses 38920 Crolles <http://www.geolithe.fr/ingenieurs-conseils/>

<sup>4</sup> Ecole Centrale Lyon – LTDS UMR 5513 : 36 Avenue Guy de Collongue 69134 Ecully Cedex

<sup>a</sup> [nathanael.savalle@uca.fr](mailto:nathanael.savalle@uca.fr), \* corresponding author

<sup>b</sup> [christine.monchal@geolithe.com](mailto:christine.monchal@geolithe.com)

<sup>c</sup> [eric.vincens@ec-lyon.fr](mailto:eric.vincens@ec-lyon.fr)

<sup>d</sup> [sten.forcioli@geolithe.com](mailto:sten.forcioli@geolithe.com)

<sup>e</sup> [pbl@civil.uminho.pt](mailto:pbl@civil.uminho.pt)

## Abstract

Dry Stone Retaining Walls are structures made of rubble stones assembled without mortar and have been present worldwide for centuries. Today, they still constitute an attractive alternative to building techniques involving higher embodied energy, such as reinforced concrete walls. This study uses a pseudo-static approach to give design recommendations to maintain this built heritage and allow its modern construction. Both non-seismic (Eurocode 7) and seismic (Eurocode 8) cases are addressed. The present work confirms that a seismic design is not critical and is therefore not required for zones with a design acceleration below 0.05g. In addition, this work highlights the significant positive effect of the stone bed inclination and the internal wall face batter. Finally, depending on the wall site conditions and the seismic zone associated with the project, general design recommendations are given to optimise the volume of stones used, which are illustrated in the case of France. These recommendations based on pseudo-static analyses are already usable in practice for low to moderate seismic areas as the required retaining wall dimensions can be easily implemented on-site. In addition, it is also shown that the actual French recommendations for these walls fully comply with Eurocode 7.

## Keywords

Masonry, Dry stone, Retaining walls, Pseudo-static, Earthquakes, Coulomb's wedge, Standards

## 29 Introduction

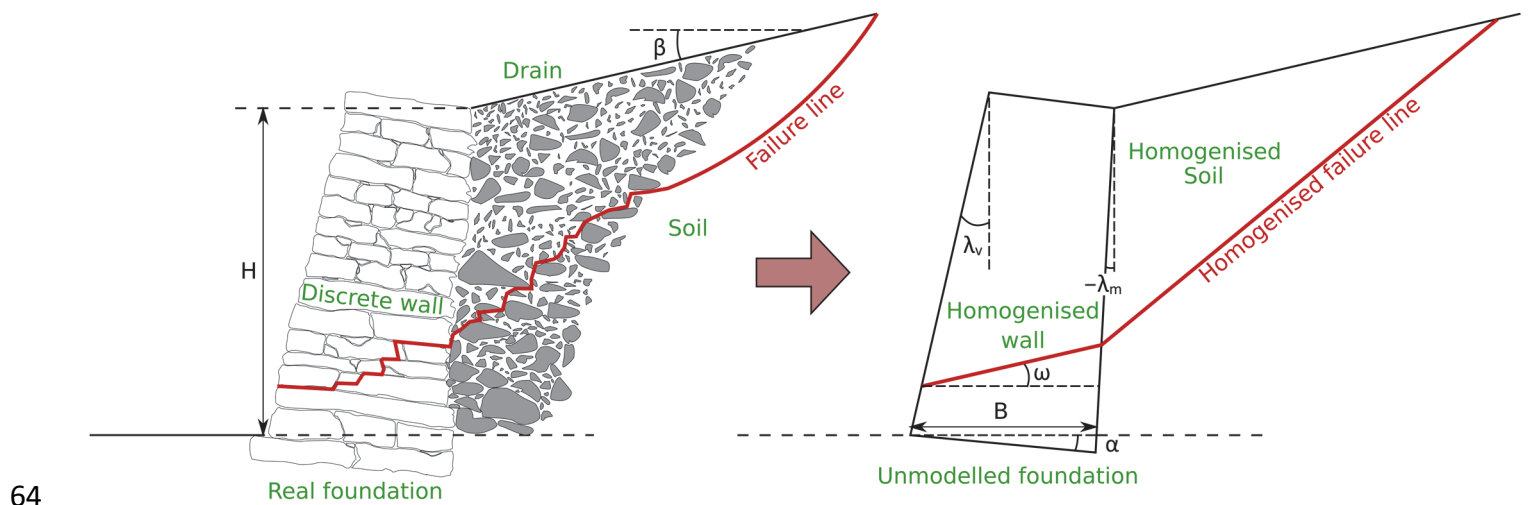
30 Dry stone structures have been built in most regions of the world, sometimes shaping typical and valuable  
31 landscapes. These vernacular structures are made of rubble stones carefully assembled by hand and without  
32 mortar. Dry Stone Retaining Walls (DSRWs) are likely to constitute the most representative part of this built  
33 heritage, allowing agricultural activities on terraces and traffic on rural roads in mountainous or sloped areas.  
34 Therefore, DSRWs play an essential economic role in these regions that benefit less from globalisation and  
35 major investments. In addition, they also hold a high cultural value, sometimes labelled by UNESCO (e.g.,  
36 Douro's Valley in Portugal or the Lavaux's Terraces in Switzerland). In fact, the art of dry stone walling,  
37 knowledge and techniques were designated as Intangible Cultural Heritage of Humanity by UNESCO in 2018.  
38 However, these structures have often faced a lack of maintenance in recent decades and require urgent repair.  
39 Given the need to preserve and repair old DSRWs, several research studies have been conducted mainly in  
40 Europe. Experimental works [1]–[3], analytical [4]–[7] and numerical studies [8]–[15] focused on the static  
41 mechanical behaviour of 2D sloped DSRWs, while other studies investigated the 3D mechanical behaviour of  
42 these walls in case of a concentrated traffic load [16]–[19]. In France, these researches led to two practical  
43 handbooks that include design rules for DSRWs retaining slopes. These are valid for any country with similar  
44 building techniques, which can be found worldwide [20], [21]. However, even though the recommendations  
45 are used in practice and recognised by the drystone masonry and civil engineering communities, they do not  
46 consider seismic action. Only a few study cases have been investigated according to the past French seismic  
47 recommendations [22], [23]. Moreover, the validation of the recommendations according to Eurocode 7 [24]–  
48 [26] has not been investigated exhaustively, even if partly considered in the latest DSRWs French handbook  
49 [21].

50 To address the seismic design of DSRWs in slopes, the authors developed a pseudo-static analytical tool based  
51 on Coulomb's wedge theory, which was validated by pseudo-static scaled-down laboratory experiments [27].  
52 The first section of this paper revised the analytical method, while the second section provides a comparison

53 with the current standards on geotechnical engineering and seismic engineering, respectively, Eurocode 7 & 8  
 54 [24]–[26], [28], [29]. Finally, following the Eurocodes, recommendations are given for designing DSRWs in areas  
 55 ranging from very low to high seismicity.

## 56 Analytical method

57 The analytical method relies on the limit-equilibrium theory under plane strain conditions (Figure 1). The DSRW  
 58 is characterised by a height  $H$ , a base width  $B$ , an external slope to the vertical of  $\lambda_v$  and an internal slope to the  
 59 vertical of  $\lambda_m$ . The bed inclination of the wall is referred to as  $\alpha$  and the backfill slope as  $\beta$ . Contrary to the static  
 60 limit-equilibrium approach of Villemus [30], the analytical method includes seismic forces modelled as  
 61 equivalent horizontal pseudo-static actions. Briefly, the pseudo-static equilibrium of a Coulomb's wedge of soil  
 62 is first computed to obtain the pseudo-static active earth pressure [31]–[33]. The wall's equilibrium is then  
 63 computed, stating the possible types of failure: an internal sliding or toppling mode [34].



65 *Figure 1: DSRW with its geometric parameterisation a): actual backfill-wall system; b): modelled backfill-wall system. The present sign convention*  
 66 *makes the internal batter ( $\lambda_m$ ) negative.*

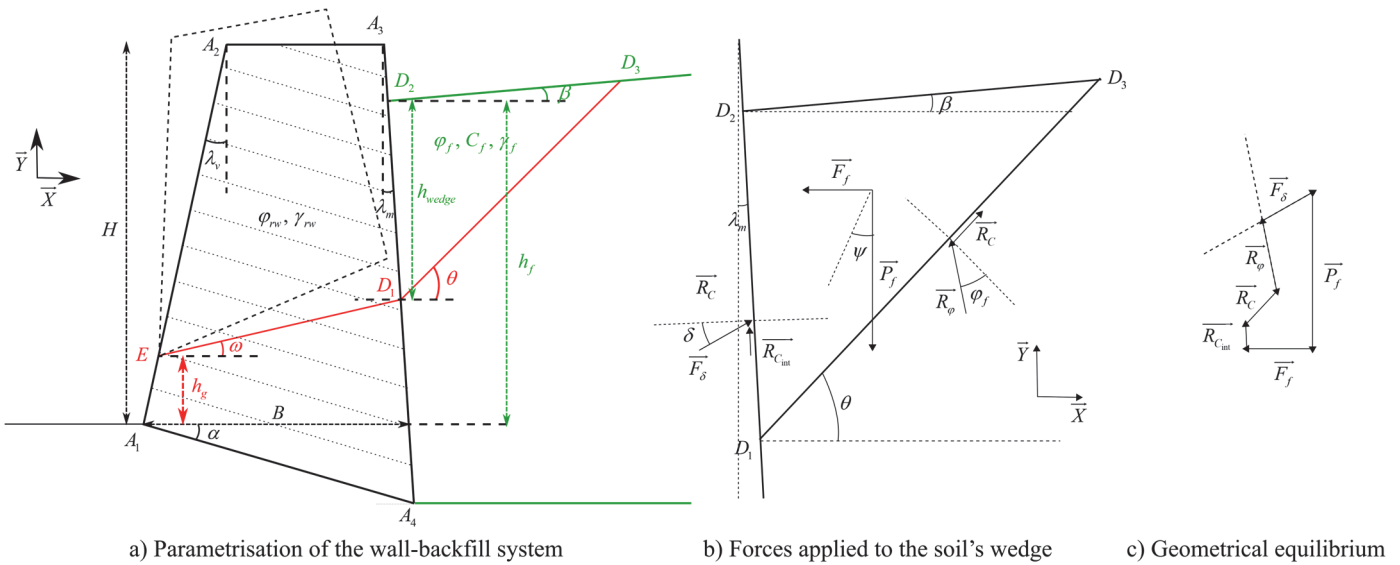
67 Figure 2 describes the backfill-wall system, with all geometrical and mechanical parameters clarified. The wall  
 68 is characterised by a homogeneous medium (Figure 1) with its homogeneous unit weight  $\gamma_{rw}$  (accounting for  
 69 voids between stones) and joint frictional angle  $\varphi_{rw}$ . Similarly, the backfill is modelled as a homogeneous  
 70 medium described by its unit weight  $\gamma_f$ , cohesion  $C_f$  and friction angle  $\varphi_f$ . Compared to other retaining

71 structures, the particularity of DSRWs lies in a failure line developing through the dry joints, which is modelled  
72 as an equivalent straight failure line with an inclination  $\omega$  (Figure 1). In practice, the inclination of this failure  
73 line from the bed joints is limited by a maximum value of  $20^\circ$ , see [27]. This inclination is also different from  
74 the homogenised inclination  $\theta$  of the failure line crossing the backfill, which mainly depends on material (soil  
75 friction and cohesion), geometrical (slope of the backfill) and seismic (pseudo-static accelerations) parameters,  
76 as explained below.

77 The mechanical system has three unknowns ( $\theta$ ,  $\omega$  and  $h_g$ ) that should be determined to compute the earth  
78 pressure  $F_\delta$ . According to the Coulomb soil's wedge theory, for each combination of these parameters, the limit  
79 equilibrium of the soil's wedge  $D_1D_2D_3$  can be calculated (Figure 2b-c) to evaluate the active earth pressure  $F_\delta$ .  
80 In particular, the weight  $P_f$  of the soil is proportional to the wedge area (triangle  $D_1D_2D_3$ ) and is applied at the  
81 gravity centre of the triangle  $D_1D_2D_3$ . Similarly, the pseudo-static action (inertial force due to the seismic  
82 motion)  $F_f$  is also proportional to the wedge area and applied at its gravity centre. The backfill frictional reaction  
83  $R_\varphi$  application point and intensity are unknown, but its orientation is given by the backfill friction angle  $\varphi_f$  since  
84 the limit-equilibrium is assumed. Similarly, the orientation, yet not the application point, of the backfill cohesive  
85 reaction  $R_C$  is known. Regarding the backfill-wall interface, the interface cohesive reaction  $R_{Cint}$  has an unknown  
86 point of application and a known orientation. The intensities of the cohesive forces ( $R_C$  and  $R_{Cint}$ ) are  
87 proportional to the cohesive strength and the length of the interface ( $D_1D_3$  and  $D_1D_2$ ). Hereafter, the interface  
88 cohesive strength ( $R_{Cint}$ ) always equals zero, as the drain directly behind a DSRW is usually made of dry  
89 cohesiveless gravel.

90 Finally, the earth pressure  $F_\delta$  has a known orientation  $\delta$  (internal face of the wall) and application point but  
91 unknown intensity. The intensity is deduced from the mechanical equilibrium of the soil's wedge (Figure 2c). In  
92 the absence of pseudo-static action  $F_f$  and cohesive resistance, the application point of the earth pressure is  
93 located at one-third of the height of the retaining structure. Then, adding cohesive effects decrease the

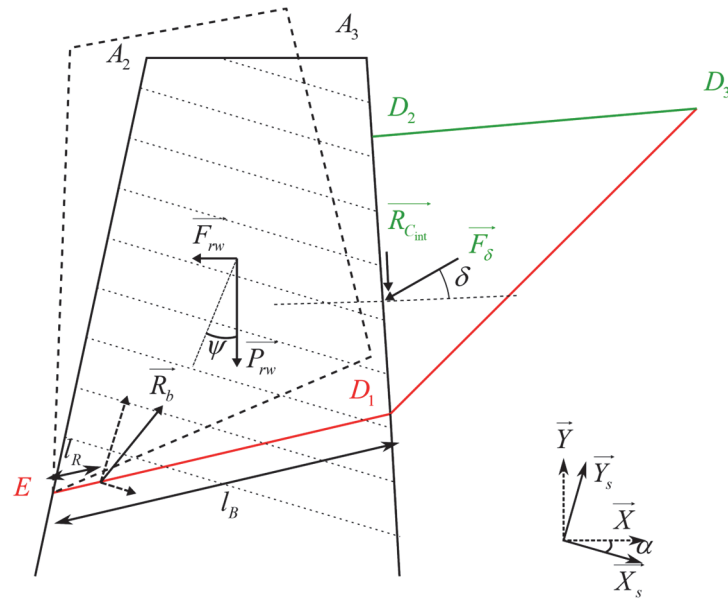
94 application point height while adding a pseudo-static action increases its height. The reader can refer to the  
 95 literature for deeper insights into the location of the application point of earth pressure in this case [34]–[36].  
 96 The analytical method also accounts for the tensile cracks that classically occur at the top of cohesive backfill  
 97 and reduce the cohesive forces ( $R_C$  and  $R_{Cint}$ ). In addition, in the present work, the presence of dead loads on  
 98 top of the backfill and saturated retained backfill [34] can be accounted for, yet not described here for brevity.



99  
 100 *Figure 2: Parametrisation of the mechanical system and geometrical equilibrium of the soil's wedge in order to compute the earth pressure  $F_\delta$ . [34]*

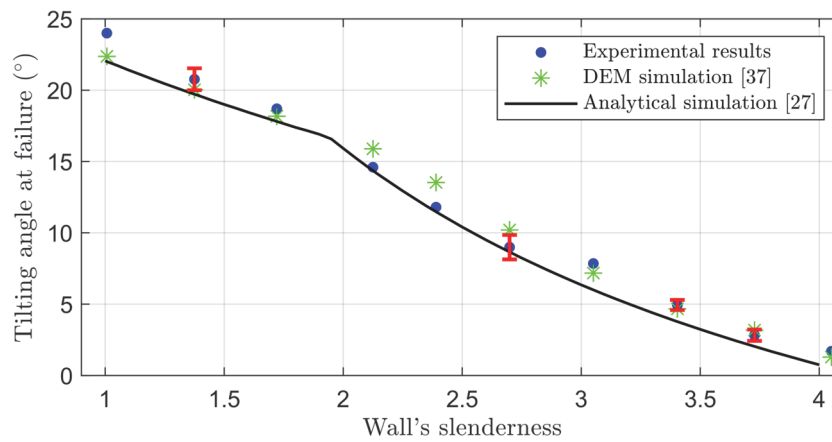
101 In a second stage of the calculation, the equilibrium of the wall itself is computed (Figure 3) including its own  
 102 weight and the pseudo-static horizontal action, applied at the centre of gravity of the studied portion of wall  
 103  $A_2A_3D_1E$ , corresponding to the part above the failure line  $D_1E$ . The interface actions  $F_\delta$  and  $R_{Cint}$  (as well as their  
 104 line of actions) are derived from the previous stage of calculation. Subsequently, the wall equilibrium is  
 105 computed in the  $X$  and  $Y$  directions to evaluate the base reaction  $R_b$ . The equilibrium in terms of momentum  
 106 gives the application point of  $R_b$ . Finally, the stability of wall portion  $A_2A_3D_1E$  is computed considering a toppling  
 107 mode of failure (e.g. application point inside the wall, i.e.  $l_b > 0$ , or any other criteria defined in the following  
 108 sections) or a sliding mode of failure. For this last point, the base reaction  $R_b$  is projected on the plane defined  
 109 by the orientation of the bed joints (axes  $X_s$  and  $Y_s$  in Figure 3), and then Mohr-Coulomb criterion is checked.

110 Note that the bed joints' orientation is updated because of the possible internal rotation of stones inside DSRWs  
 111 (see [34] for more details). Finally, the unknowns of the system ( $\theta$ ,  $\omega$  and  $h_g$ ) are optimised for each failure  
 112 mode to find the most critical situation for the criterion checked. Several iterations involving the base width  $B$   
 113 of the wall allows to identify the minimum  $B$  value that barely satisfies the stability criteria.



114  
 115 Figure 3: Equilibrium of the dry stone retaining wall [34]

116 The method has been validated on scaled pseudo-static experiments on a tilting table, using dry joint brick  
 117 retaining walls retaining a sandy backfill [27]. Figure 4 gives the results, showing that the developed pseudo-  
 118 static approach is as precise as more sophisticated Discrete Element Modelling (DEM) simulations [37].



119  
 120 Figure 4: Comparison of DEM simulation, analytical simulation and experimental tilting tests [37]

121 As additional validation, the analytical method was used to model two sets of experimental campaigns carried  
 122 out on full-scale DSRWs with 1) a hydrostatic load [1]; 2) a dry backfill load, as displayed in Figure 5 [2], [3].  
 123 Table 1 describes the geometric and mechanical parameters of the experiments, along with the analytical  
 124 results, which are in excellent agreement for both campaigns. Moreover, the developed analytical approach  
 125 provides a similar level of accuracy to the results of Villemus *et al.* [1] and Colas *et al.* [6], [38].



126  
127 Figure 5: Experimental toppling failure obtained by Colas [39]

128 Table 1: Parameters of the full-scale DSRWs experimental campaigns from [1]–[3]. Experimental and analytical results are also given.

Name*	V1l	V2l	V3l	V4l	V5s	C1g†	C2s	C3s	C4l
<b>Geometrical parameters</b>									
Height H (m)	2	1.95	4	2	4.25	2.5	2.5	2.5	2.5
Base width B (m)	0.9	0.91	1.8	0.9	1.8	0.6	0.6	0.7	0.65
External batter $\lambda_v$ (%)	15	0	15	12	15	6	6	6	6
Beds inclination $\alpha$ (°)	0	0	0	4	8.5	3.4	3.4	9.1	9.1
Backfill slope $\beta$ (°)	NA	NA	NA	NA	NA	26.4	31.7	32.6	34.9
<b>Mechanical parameters</b>									
Wall weight (kN/m <sup>3</sup> )	15.4	14.9	15.7	15.7	18.0	21.0	20.0	20.0	21.8
Stone friction (°)	36	36	36	36	28.5	27	25	25	35
Internal rotation (°) ‡	5	5	5	5	5	5	5	5	5
Soil weight $\gamma_r$ (kN/m <sup>3</sup> )	NA	NA	NA	NA	NA	14.9	14.9	14.9	14.9
Soil friction $\phi_r$ (°)	NA	NA	NA	NA	NA	37.7	37.7	37.7	37.7
<b>Experimental results</b>									
Critical height (m)	1.74	1.9	3.37	1.94	3.62	>2.1 7	2.41	2.96	2.95
Failure mode (S/T)	S	S/T	S	S/T	S	NA	S/T	T	T
<b>Analytical results</b>									
Critical height (m)	1.73	1.84	3.48	1.86	3.68	2.86	2.69	3.02	2.82
Failure mode (S/T) §	S	S/T	S	S/T	S	T	S/T	T	T

Difference to exp.	-1%	-3%	+3%	-4%	+2%	NA	+11%	+2%	-4%
--------------------	-----	-----	-----	-----	-----	----	------	-----	-----

\* V refers to Villemus [1] with hydrostatic loading and C to Colas [2], [3] with backfill loading, while *l* refers to limestone blocks, *s* to schist blocks and *g* to granite blocks.

† This experiment failed. However, the wall resisted at least a loading corresponding to a backfill height of 2.17m.

‡ This information is based on experimental results, using a default value. Details can be found in [1]–[3] for the experiments and in [34], [40] for the analytical method.

§ A combined sliding-overturning failure has been defined if the critical theoretical heights of the two failure modes were within a range of  $\pm 5\%$ .

## 129 Design of DSRWs following Eurocodes

130 The present section aims at designing DSRWs using the analytical method and the partial safety factors (actions,  
131 material properties and resistance) from Eurocode 7 and 8 [24]–[26], [28]. First, it is emphasised that in a  
132 seismic context, a pseudo-static method (like the one presented above) will never accurately predict the true  
133 time evolution of the dynamic response or resistance of a real DSRW during an earthquake. Therefore, it is only  
134 used as a simplified design method proposed by Eurocode 8 to give fast seismic assessment of retaining walls.  
135 No partial safety factor related to the method is considered since no constant bias has been found in the  
136 validation processes between theoretical and experimental results. Moreover, only the wall's internal sliding  
137 and toppling failures are considered: the bearing capacity of the foundation soil at ultimate or serviceability  
138 limit states are assumed not to be reached. Similarly, the passive soil is considered infinitely rigid, which is  
139 reasonable according to Alejano *et al.* [5]. Finally, liquefaction and the failure of the entire soil slope are  
140 disregarded. Table 2 presents the safety factors used for the computations as well as those from the French  
141 professional rules, which are similar [21].

142 Regarding non-seismic verifications, the Ultimate Limit State Equilibrium (ULS EQU), the  
143 Structural/Geotechnical Ultimate Limit State with the second approach (ULS STR/GEO), see [41], and the  
144 Serviceability Limit State (SLS) are examined. The Ultimate Limit State (ULS SEISM) is applied for the seismic  
145 verification.



	Eurocode 7 [24]				French professional rules [21]
	ULS			SLS	
	EQU	STR/GEO	SEISM		
<b>Safety factors for actions</b>					
Favourable weight actions factor ( $\gamma_{G, fav}$ )	0.9	1	1	1	1
Unfavourable weight actions factor ( $\gamma_{G, unfav}$ )	1.1	1.35	1	1	1.35
<b>Safety factors for material properties</b>					
Drained soil friction angle factor ( $\gamma_{\phi'}$ )	1.25	1	1.25	1	1
Drained soil cohesion factor ( $\gamma_{c'}$ )	1.25	1	1.25	1	1.25
<b>Safety factors for resistances</b>					
Sliding factor ( $\gamma_{R, h}$ )	1	1.1	1	NA	1
Toppling factor ( $\gamma_{R, v}$ )	1	NA	1	NA	1
Eccentricity factor ( $1 - 2e/B$ )	NA	1/15	NA	1/2	1
Model resistant factor ( $\gamma_{R, d}$ )	1	1	1	1	1.2

147

148 For the toppling verification of the SLS and the ULS STR/GEO, the design criterion to satisfy corresponds to the  
149 maximum eccentricity (noted  $e$ ) of the transmitted load through the wall, as stated in Eurocode 7 [25], [26]. In  
150 the context of the ULS EQU and SEISM verifications, the partial safety factors  $\gamma_m$  ( $\gamma_{\phi'}$  and  $\gamma_{c'}$ ) for the materials  
151 are only applied to the backfill soil properties and not to the friction between blocks (as mentioned in [41]–  
152 [43]). The friction between blocks is linked to the wall resistance, thus to the resistance safety factor  $\gamma_R$ . As a  
153 consequence, applying a safety factor for the block material (block-block friction) would penalise twice the  
154 same parameters, which is not in agreement with the framework of Eurocodes. Moreover, in the seismic  
155 verification (ULS SEISM), the safety factors for materials are linked to the degradation of the shear strength of  
156 soils at high strain and/or in the presence of pore pressures. These are unlikely to occur for dry block-block  
157 joints [42]–[44].

#### 158 Non-seismic case

159 Computations discarding the seismic action are carried out on five walls, whose main characteristics are  
160 presented in Table 3. The walls are built of stones with geological natures representative of European and, in  
161 particular French, geology (molasse or marl sandstone, schist, limestone and granite). They include typical

162 variations of essential DSRW properties (geometrical shape and soil resistance). Note that their height is typical  
 163 of relatively high DSRWs. The backfill-wall interface friction angle  $\delta$  is equal to the soil friction angle, given the  
 164 dry gravel drain placed behind each DSRW [2], [3]. Both the internal batter  $\lambda_m$  and the stone bed inclination  $\alpha$   
 165 are initially equal to zero. The minimum required (bottom) widths for the walls given by the Eurocodes are then  
 166 computed and compared to the recommended widths from ENTPE (Eds) *et al.* [21].

167 *Table 3: Main characteristics and required widths of five typical DSRWs according to Eurocode 7 (non-seismic case) criteria; maximum values are*  
 168 *given in bold. Comparisons with the recommendations of ENTPE (Eds) et al. [21] are also given. Each column heading displays the critical failure mode*  
 169 *(T: toppling; S sliding). Granite DSRWs have similar properties as schist walls, and the values shown for schist can be used.*

	Wall 1 (T) Molasse	Wall 2 (S) Schist	Wall 3 (T) Limestone	Wall 4 (S) Schist	Wall 5 (T) Limestone
<b>Mechanical &amp; geometric properties</b>					
Height H (m)	2.5	2.5	2.5	2.5	2.5
External batter $\lambda_v$ (%)	0	10	20	10	0
Backfill slope $\beta^*$ (°)	0	0	0	0	10
Wall unit weight $\gamma_{rw}$ (kN/m <sup>3</sup> )	16	20	20	20	20
Blocks friction $\phi_{rw}$ (°)	36	28	36	28	36
Backfill unit weight $\gamma_f$ (kN/m <sup>3</sup> )	20	20	20	20	20
Backfill cohesion $C_f$ (kPa)	0	0	0	5	0
Backfill friction $\phi_f$ (°)	30	30	25	25	30
Interface friction $\delta$ (°)	30	30	25	25	30
<b>Non-seismic design: wall base widths</b>					
ULS EQU (Sliding)	0.57m	<b>0.83m</b>	0.85m	<b>0.68m</b>	0.54m
ULS EQU (Toppling)	<b>0.83m</b>	0.77m	<b>0.90m</b>	0.51m	<b>0.81m</b>
ULS STR-GEO (Sliding)	0.51m	0.77m	0.82m	0.63m	0.47m
ULS STR-GEO (Toppling)	0.76m	0.71m	0.84m	0.30m	0.74m
SLS (Eccentricity)	<b>0.89m</b>	0.78m	<b>0.91m</b>	0.30m	<b>0.86m</b>
ENTPE (Eds) et al. [21]	<b>0.91m</b>	<b>0.85m</b>	<b>1.00m</b>	<b>0.75m</b>	<b>0.88m</b>
Absolute difference	2%	2%	9%	9%	2%

170  
 171 \* The slope inclination refers to the backfill directly retained by the wall and not the global slope of the site.

172 The recommendations from ENTPE (Eds) *et al.* [21] are very close to the maximum value recommended by the  
 173 Eurocode standards with slightly larger and conservative values: on average +5% and maximum +10%  
 174 difference. The most critical limit state and the corresponding failure mode differ according to the studied walls,  
 175 justifying the consideration of all possible limit states. Finally, even if only five case studies are shown for  
 176 brevity, the authors carried out a more comprehensive set of typical walls with identical conclusions.

179 The same walls are assessed according to Eurocode 8 [29], [44], assuming their design is provided by the most  
 180 non-seismic critical case mentioned above. Keeping all other geometrical parameters constant, the extra-width  
 181 required to withstand the seismic loading is computed (see Table 2 for the associated partial safety factors).  
 182 Here, the authors recall that this section does not aim to describe precisely the dynamic behaviour of DSRWs  
 183 against earthquakes but aims to provide a safe design width for DSRWs built in a seismic context. For this  
 184 reason, the simplified pseudo-static modelling strategy is considered. The following equations give the pseudo-  
 185 static design accelerations (horizontal  $a_h$  and vertical  $a_v$ ):

$$(1) \quad a_h = \frac{a_{gR} * S * S_T * \gamma_I}{r}, \quad a_v = 0.5 * a_h$$

186 where  $a_{gR}$  is the reference acceleration for the considered seismic zone;  $S$  is the soil amplification factor (the  
 187 maximum value being  $S = 1.8$ );  $S_T$  is the topographic amplification coefficient;  $\gamma_I$  is the importance coefficient  
 188 of the structure; and  $r$  is the seismic behaviour factor [29]. The latter parameter considers the wall's ability to  
 189 move during the seismic motion and dissipate seismic energy before collapsing [28], [44].

190 Scaled-down experiments on a shaking table suggested a conservative value of  $r = 1.5$  [45], corresponding to  
 191 walls able to handle small movements before collapsing according to Eurocode 8 [28]. In addition, numerical  
 192 simulations using DEM approach have concluded that  $r = 1.5$  was indeed conservative enough for the French  
 193 seismicity [46]. In fact, after a numerical validation step using scaled-down experiments with dynamic time-  
 194 history analyses, the numerical model was applied to full-scale structures with various dynamic time-history  
 195 analyses (signal and backfill-wall parameters). Then, comparing the obtained numerical resistance and the  
 196 estimated (analytical) pseudo-static resistance, the seismic behaviour factor  $r$  for each configuration was  
 197 determined. Combining all the results, a mean value of  $r = 2.0$  and a minimum value of  $r = 1.8$  have been found.  
 198 Therefore, a conservative recommended value of  $r = 1.5$  was proposed since Eurocode only advises three values  
 199 for  $r$  namely 1, 1.5 and 2. Even though this study has focused on the French case with moderate seismicity, the

200 obtained outcome is considered acceptable elsewhere in Europe, especially given the safety margin taken at  
201 each step in [46]. In all analyses, the studied DSRWs are assumed to belong to the normal importance class.  
202 Particular conditions that rarely occur on-site are excluded (e.g., walls near very high buildings, highways,  
203 hospitals or energy facilities). It means that the importance coefficient  $\gamma_I$  is lower than (or equal to) 1, which  
204 also implies no topographic amplification ( $S_T = 1$ ). Depending on the reference acceleration  $a_{gR}$ , the most critical  
205 design acceleration reads:

206

$$(2) \quad a_{h,max} = \frac{a_{gR} * 1.8}{1.5} = a_{gR} * 1.2, \quad a_{v,max} = 0.5 * a_{h,max} = a_{gR} * 0.6$$

207 Figure 6 depicts the extra-width required to fulfil a seismic design compared to the previously non-seismic  
208 design for each of the five walls (Table 3). Eurocode 8 states that seismic design is not required below a  
209 threshold of  $a_h = 0.05g$  [29]: actually, the current calculations show that even if accounted for, the seismic case  
210 is not critical for the wall stability (Figure 6). For higher design accelerations, walls sensitive to a sliding failure  
211 (case of schist wall, Figure 6a) tend to have larger required extra-widths than those sensitive to a toppling  
212 failure (Figure 6b-c). Finally, for high seismic hazard regions in Europe and France, see Figure 7 ( $a_h = 0.25 - 0.4g$ ),  
213 extra-widths reach very high values (+200%), reflecting the inaccuracy of the pseudo-static method for high  
214 reference accelerations, which provides unpractical recommendations for on-site works. Here, it is noted that  
215 wall disintegration is not considered, meaning that in high seismicity areas, additional prevention actions may  
216 be required.

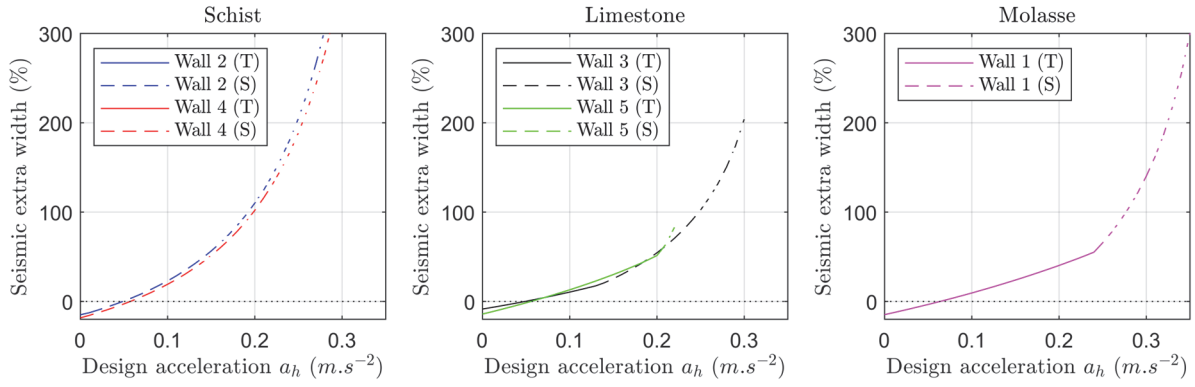
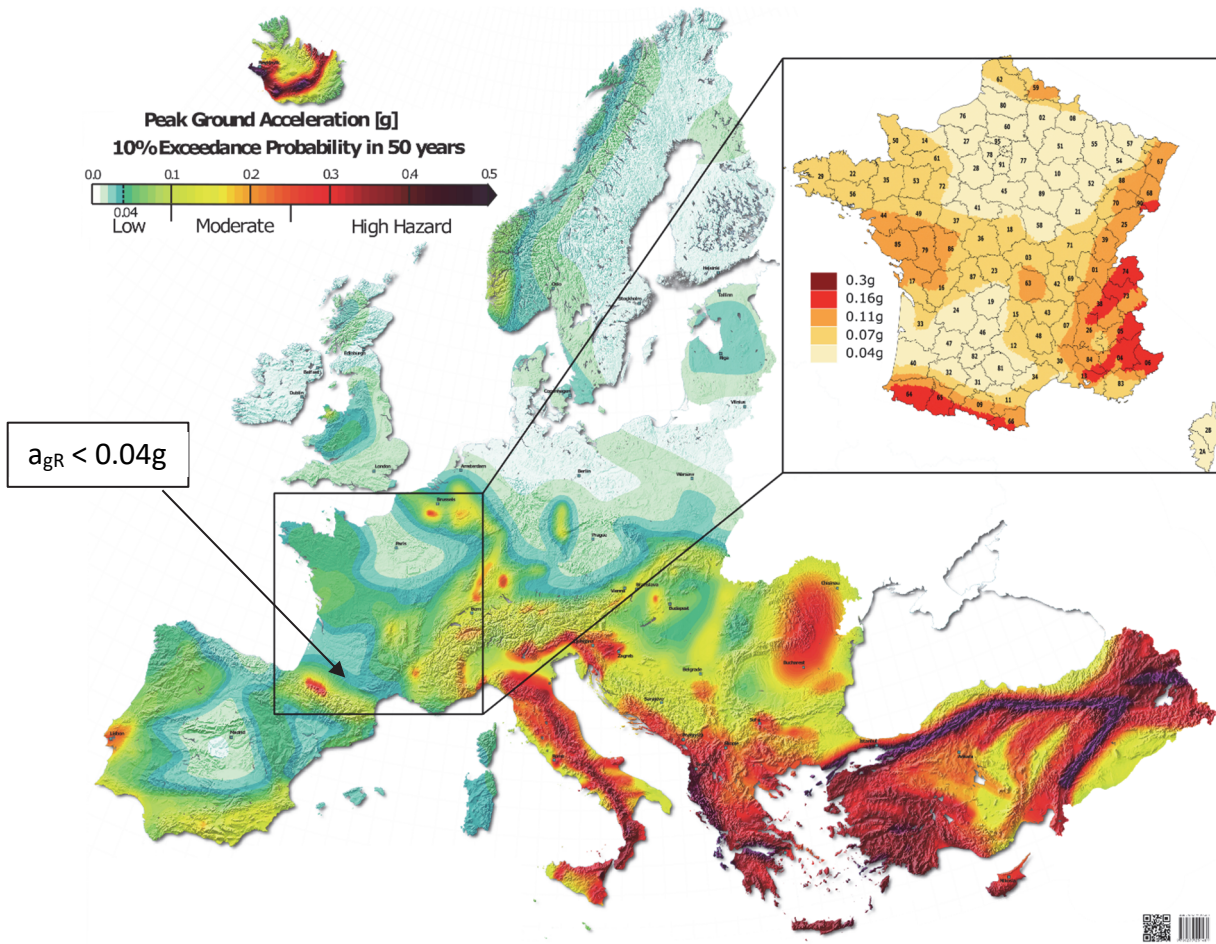


Figure 6: Extra-width required by a seismic design compared to a non-seismic design for the studied walls. Walls are presented according to the type of stone used; a) schist; b) limestone; c) molasse (marl sandstone).

A larger set of walls was analysed to obtain more general results. Walls geometries are still given in Table 3, but each geometry uses three different types of stone (schist, limestone, and molasse). Additionally, the analysis considers three typical bed inclinations  $\alpha$  ( $0^\circ$ ,  $10\%=5.7^\circ$  and  $20\%=11.3^\circ$ ) for each wall to improve the sliding resistance of DSRWs [2], [30], [47], [48]. Figure 8 gives the maximum (and mean) required extra-widths for DSRWs built with different kinds of stone depending on the stone bed inclination  $\alpha$ . Here, the local peaks are related to vertical asymptotes for a peculiar response: when the design acceleration  $a_h$  equals  $a_{h, critical}$  (Eq. 3), the whole retained soil slope loses its static equilibrium leading to infinite forces impossible to be sustained by the wall. Hence, the pseudo-static design requires huge wall widths close to this critical acceleration.

$$(3) \quad a_{h,critical} = \frac{\sin(\varphi_r - \beta) + \frac{c_r \cos \varphi}{\gamma_r * H \cos \beta}}{\cos(\varphi_r - \beta) + 0.5 * \sin(\varphi_r - \beta)}$$



228

229

230

Figure 7: European map of reference acceleration  $a_{gR}$  (return period of 475 years) according to Giardini et al. [49]. The threshold  $a_{gR} = 0.04g$  is also highlighted in the legend. National seismic zonation maps in Eurocode 8 currently differ from this map.

231

232

233

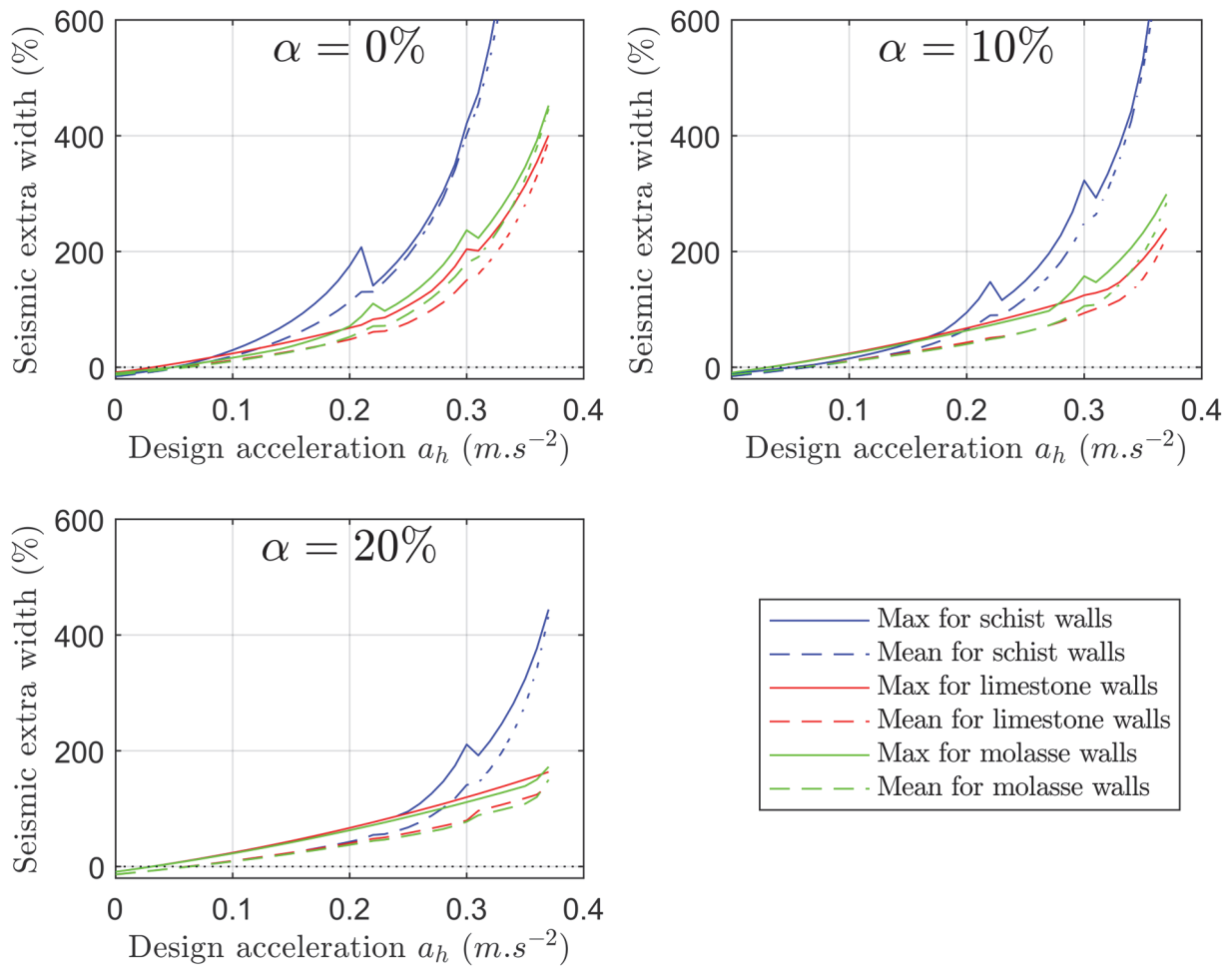
234

235

236

237

For clarity, the maximum and mean values displayed in Figure 8 ignore walls around and after their critical acceleration  $a_{h, critical}$ , yet still resulting in small visible local peaks. For example, the first peaks for a design acceleration of about 0.22g observed in Figure 8 correspond to Wall 5, the only case with a non-zero backfill slope  $\beta$ . Therefore, in practice, one should prefer to build a higher wall with a flat retained backfill than a smaller wall with an inclined backfill, especially in high seismic hazard regions. Finally, Eq. 3 highlights the inherent limitation of the design approach proposed by Eurocodes, which does not apply for high design acceleration  $a_h$ , basically larger than 0.25-0.4g depending on the parameters of the backfill.



238

239

240

Figure 8: Maximum (continuous line) and mean (dashed line) required extra-widths for the studied DSRWs depending on the type of stone and the stone beds inclination  $\alpha$ : a)  $\alpha=0\%$ ; b)  $\alpha=10\%$ ; c)  $\alpha=20\%$ .

241

242

243

244

245

246

247

248

Analysing Figure 8, it is noted that increasing the stone bed inclination is very efficient in reducing the extra-widths according to a pseudo-static design, although this parameter was not integrated into the non-seismic French recommendations [20], [21]. Table 4 details the maximum required extra-widths for each bed inclination according to different reference accelerations ( $a_{gR}$ ) representative of Europe. A non-exhaustive description of the concerned regions is also given for each reference acceleration. For most western, northern, and eastern Europe, where the reference acceleration is smaller than  $a_{gR} = 0.11g$  (low to medium seismicity), the maximum required extra-width reaches about 50%. If the wall is more resistant to sliding (not built with schist or with a non-zero bed inclination), the maximum extra-width decreases to about 35%. Finally, for reference

249 accelerations larger than 0.25g, due to the inherent approximations of the pseudo-static approach, the  
 250 maximum extra-widths exceed 100% of the non-seismic design which seems non reasonable in practice. For  
 251 these cases, the pseudo-static modelling approach may also be inadequate, given the weak consideration of  
 252 dynamics and the fact that wall disintegration is ignored.

253 *Table 4: Maximum extra-widths for DSRWs required by a pseudo-static seismic design compared to a non-seismic design depending on the reference*  
 254 *acceleration ( $a_{gR}$ ). The analysis only covers DSRWs belonging to the normal class of importance ( $\gamma_I \leq 1.0$ ). According to the seismic hazard map of*  
 255 *European countries, the second column gives the corresponding regions of each reference acceleration. The reader is referred to Figure 7 and Figure*  
 256 *8.*

Reference acceleration $a_{gR}$ (design acceleration $a_{h,max}$ )	Corresponding regions in Europe	Max (and mean) extra widths		
		$\alpha = 0\%$	$\alpha = 10\%$	$\alpha = 20\%$
0.04g (0.05g)	Most Northern Europe (up to France, Germany and Poland) + Mainland Spain	6% (0%)	6% (0%)	6% (0%)
0.06g (0.07g)	Most North-Eastern Europe; first seismic zone of many countries	13% (4%)	13% (2%)	13% (2%)
0.11g (0.13g)	Most Iberia; most Northern Europe up to the north of Italy and the north of Croatia	56% (26%)	36% (19%)	36% (18%)
0.16g (0.19g)	All Northern Europe; most Eastern Europe; first seismic zones of all European countries	>100% (63%)	77% (44%)	62% (37%)
0.20g (0.24g)	All Europe except localised areas (Iceland, Portugal, Spain) and high seismic regions (Croatia-Italy-Slovenia; Bosnia-Croatia-Greece-Serbia; Bulgaria-Romania; Cyprus-Turkey)	>100% ( $\approx$ 100%)	>100% (72%)	87% (55%)
0.25g (0.29g)	All Cyprus, Slovenia; almost all Bosnia, Bulgaria, Croatia, Greece, Italy, Romania	>100% (>100%)	>100% (>100%)	>100% (88%)
>0.25g (>0.29g)	Localised zones in Iceland; rest of Bosnia, Bulgaria, Croatia, Greece, Italy, Romania, and Turkey	>100% (>100%)	>100% (>100%)	>100% (>100%)

257  
 258 conclusion, the systematic use of a stone bed inclination  $\alpha$  is recommended. Whenever possible, an external  
 259 batter equal to the stone bed inclination to facilitate the construction process is also suggested. For low to  
 260 medium seismic regions ( $a_{gR} < 0.11g$ ), a stone bed inclination  $\alpha$  of 10% is suitable, whereas, for larger seismic  
 261 hazards ( $a_{gR} \cong 0.16-0.2g$ ), a value of 20% can help to reduce the required extra-widths significantly.

### 262 *French case study*

263 This section provides a more detailed case study for France, chosen as an illustrating example of low to medium  
 264 seismicity European countries. The section helps to understand the trends and practical seismic design for  
 265 DSRWs, depending on three different but typical cases for the backfill-wall condition. The first case (MAX)  
 266 corresponds to the previous European study, i.e., large amplification for the soil ( $S = 1.8$ ) and a standard  
 267 construction (importance factor  $\gamma_I = 1.0$ ). The second (ROCK) represents the most critical case when the DSRW  
 268 is directly founded on the bedrock ( $S = 1.0$ ), considered a reference case for foundation conditions. The last one  
 269 (RURAL) corresponds to walls of less importance ( $\gamma_I = 0.8$ ), built far from any road or building. In practice,



270 according to the French regulations, these specific cases (RURAL) are not subjected to seismic regulations.  
 271 However, this work gives reference values, which are helpful for DSRWs stakeholders. These three  
 272 configurations are analysed according to the four seismic zones of metropolitan France ( $a_{gR} = 0.04, 0.07, 0.11$   
 273 and  $0.16g$ ), leading to a total of 12 case studies (Table 5).

274 *Table 5: Horizontal seismic design accelerations  $a_h$  for different critical cases (as a proportion of  $g = 9.81m \cdot s^{-2}$ ). The vertical acceleration  $a_v$  is*  
 275 *systematically taken equal to  $0.5 \cdot a_h$ .*

	$a_{gR}$	MAX	RURAL	ROCK
Formulas used to compute $a_h$	-	$a_{h, \max} = a_{gR} \cdot 1.20$	$a_{h, \text{rural}} = a_{gR} \cdot 0.96$	$a_{h, \text{rock}} = a_{gR} \cdot 0.67$
Very Low Seismic zone (S1)	0.04g	0.05g	0.04g	0.03g
Low Seismic zone (S2)	0.07g	0.09g	0.07g	0.05g
Moderate Seismic zone (S3)	0.11g	0.13g	0.11g	0.07g
Mean Seismic zone (S4)	0.16g	0.20g	0.16g	0.11g

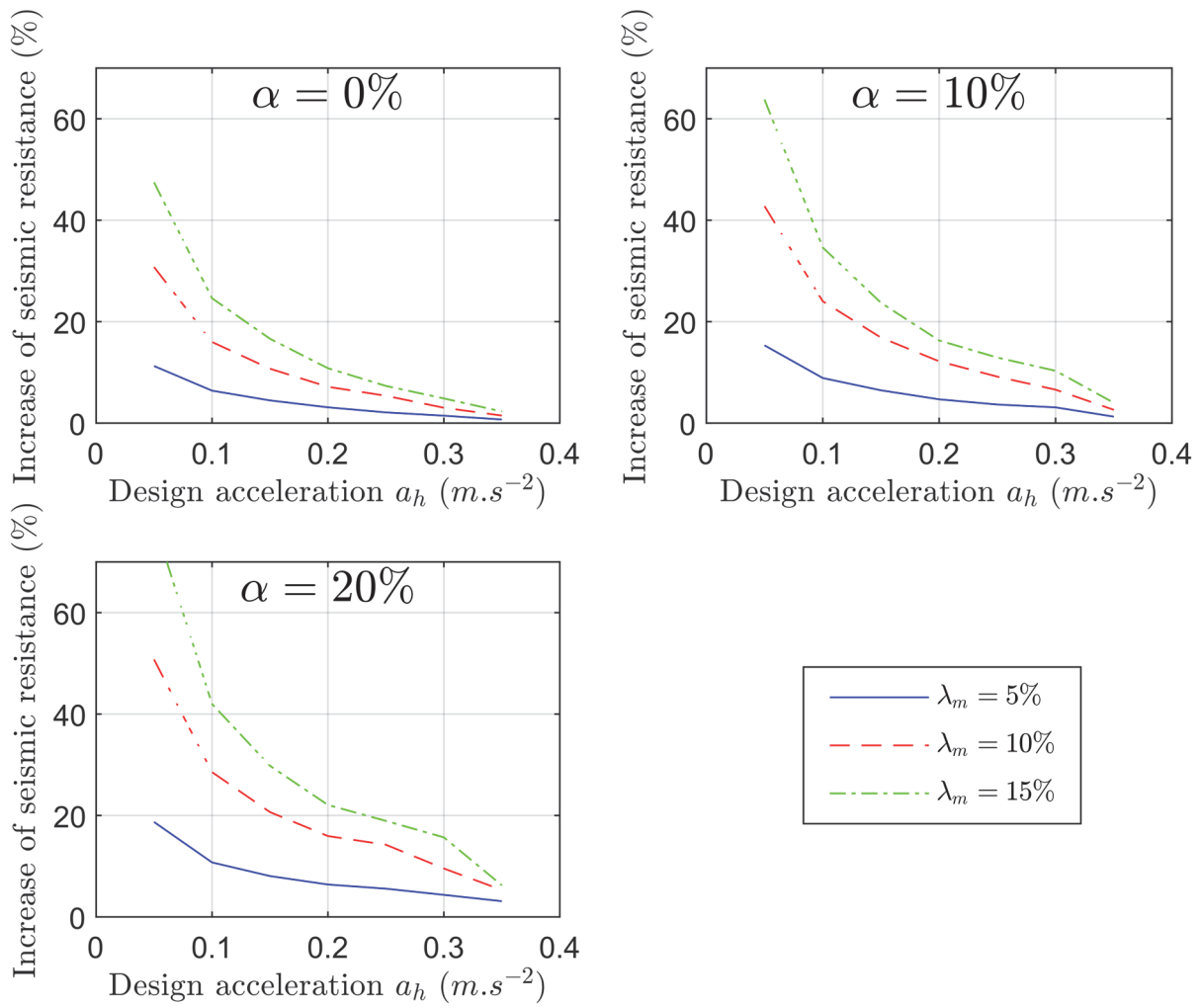
276  
 277 Table 6 sums up the maximum (and mean) extra-widths (among the different walls and stones type) obtained  
 278 for each seismic situation depending on the stone bed inclinations. In seismic zones S1 to S3, one can again  
 279 note that bed inclination  $\alpha$  dramatically impacts the results; however, a bed inclination of 20% does not provide  
 280 a significant increase in resistance compared with an inclination of 10% (see also Figure 8b-c). Therefore, as  
 281 usual in the South of France, an inclination of the stone bed of 10% is recommended: seismic design requires  
 282 no more than 40% extra-width (compared to a non-seismic design). In seismic zone S4, walls built with a stone  
 283 bed inclination of 10% require an extra-width of 90%, which induces substantial extra costs for the wall  
 284 construction. In this case, one should either use a steeper bed inclination or conduct a specific analytical  
 285 computation to optimise the geometry of the DSRW. However, if the wall is built far away from roads and  
 286 buildings (RURAL) and with an inclination bed of 10%, the maximum expected extra-width only reaches 50%.  
 287 On the contrary, if the wall is directly founded on the bedrock (ROCK), the seismic required extra-width drops  
 288 to a maximum of 30%. If both conditions are fulfilled (RURAL & ROCK), the required extra-widths do not exceed  
 289 20% (case not addressed in Table 6). Finally, the general recommendations of Table 6 (maximum values) can

290 be readily used for practical non-seismic and seismic design of DSRWs without requiring more detailed  
 291 computations.

292 *Table 6: Influence of the stone bed inclination  $\alpha$  on the extra width required for seismic design. Maximum values, together with average values in*  
 293 *parentheses, are given.*

	$\alpha = 0\%$	$\alpha = 10\%$	$\alpha = 20\%$
ROCK-S1 (0.03g)	0% (0%)	0% (0%)	0% (0%)
RURAL-S1 (0.04g)	2% (0%)	2% (0%)	3% (0%)
ROCK-S2 / MAX-S1 (0.05g)	6% (0%)	6% (0%)	6% (0%)
RURAL-S2 (0.07g)	12% (4%)	12% (3%)	12% (3%)
ROCK-S3 (0.07g)	15% (6%)	15% (4%)	15% (4%)
MAX-S2 (0.09g)	20% (9%)	19% (7%)	19% (7%)
RURAL-S3 / ROCK-S4 (0.11g)	36% (17%)	27% (13%)	27% (12%)
MAX-S3 (0.13g)	61% (28%)	39% (21%)	39% (19%)
RURAL-S4 (0.16g)	89% (40%)	49% (29%)	48% (25%)
MAX-S4 (0.20g)	>100% (67%)	87% (47%)	67% (39%)

294  
 295 As already noted, specific analytical computations should be carried out for the situation MAX-S4 or more  
 296 critical seismic implantations instead of using the general approach with the maximum values displayed in Table  
 297 6. More specifically, one should pay attention to specific parameters of the DSRW in the design that plays a  
 298 critical role in the seismic computation (see full details in [40]). Apart from the positive influence of the stone  
 299 bed inclination and the negative effect of the retained slope angle already highlighted, a positive internal wall  
 300 batter is recommended (this is the case of a self-stable wall). To support this recommendation, Walls 1 to 5  
 301 (with various stone types and bed inclinations) have been designed to withstand a specific seismic acceleration  
 302 (0.05g, 0.10g ... and 0.35g). In a second step, each wall section geometry has been modified, adding an internal  
 303 batter ( $\lambda_m = 5\%$ , 10% and 15%) but keeping the same surface area as before. It means that the total volume of  
 304 stones used in that case is the same but that the geometry of the wall section is different (i.e., with a larger  
 305 width at the base). Finally, the maximum acceleration withstood by the walls with an internal batter is  
 306 compared to the maximum acceleration found for those without the batter (Figure 9). The curves correspond  
 307 to the average values found throughout the different walls and stones. Only positive values have been found,  
 308 meaning a systematic improvement of the seismic resistance when adding an internal batter. This improvement  
 309 is particularly significant for walls with non-zero stone bed inclination and low (S2) to moderate (S3) seismic  
 310 hazard regions.



311

312

Figure 9: Effect of the internal batter  $\lambda_m$  (keeping the same area for the wall section) on the seismic resistance of a DSRW for different bed inclinations

313

a)  $\alpha=0\%$ ; b)  $\alpha=10\%$ ; c)  $\alpha=20\%$ .

314

To conclude, in zone S2, no DSRW extra-width is required to fulfil a seismic design if both an inclination bed of 10% and an internal batter of at least 10% are used. This means that an adequate choice for the wall geometry compensates for the required extra resistance required to satisfy a seismic design in case of low seismicity.

317

## Conclusions

318

The present study addresses non-seismic and seismic designs of Dry Stone Retaining Walls (DSRWs) according to the European standards (Eurocodes) used for conventional retaining walls while proposing an adapted methodology (e.g. including internal failure of DSRW). It has been shown that the current French recommendations for the non-seismic design of DSRWs comply with Eurocode 7 (geotechnical engineering)

321

standards being slightly more conservative than the latter. Moreover, in very low seismic zones ( $a_h < 0.05g$ ), non-seismic limit states are the most critical states for the design of DSRWs, which confirms that a seismic design is not required in these regions [29]. This is generally not the case in zones of higher seismicity where the seismic design according to Eurocode 8 (seismic engineering) standard is almost always the most critical.

The study revealed different geometrical optimisation options for DSRWs. It is highly recommended to use systematically: i) a bed inclination of at least 10%; ii) a flat retained backfill; iii) and a positive internal batter of at least 10%. These three geometric parameters have a significant impact on seismic design. If these recommendations are followed in low seismic zones (up to  $a_h = 0.08g$ ), there is also no increase in dimensions to fulfil a seismic design.

The pseudo-static approach generally gives practical global recommendations for low to moderate seismic hazard zones (up to  $a_h = 0.2g$ ). In addition, a specific geometrically optimised (as stated above) pseudo-static design can still produce affordable recommendations in more critical cases (up to  $a_h = 0.3g$ ). However, for higher design acceleration or particularly critical cases, the pseudo-static approach for the seismic design leads to values higher than 50% for the extra-widths. In this case, dynamic time history computations are recommended to obtain more accurate results that account for wall disintegration failure. Indeed, this failure mode may be critical for high seismicity areas, particularly if combined with poor execution conditions.

Finally, as an example illustrating European countries, France is used as a case study of seismic design applied to DSRWs in low to moderate seismicity areas. In metropolitan France, where many DSRWs can be found, the expected extra-width provided by seismic design does not exceed 40% for walls located in low seismic zones presenting a stone bed inclination of 10%, in case the foundation is not on the bedrock. In the same conditions, walls built in moderate seismic hazard zones need either a stone bed inclination of 20% or a specific analytical computation to optimise the section. Finally, walls directly founded on the bedrock, in the case of low and moderate seismicity areas, require a maximum of 30% extra width to fulfil a seismic design.

## 345 Funding

346 This work was partly financed by FCT / MCTES through national funds (PIDDAC) under the R&D Unit Institute  
347 for Sustainability and Innovation in Structural Engineering (ISISE), under reference UIDB / 04029/2020. This  
348 study has also been partly funded by the STAND4HERITAGE project (New Standards for Seismic Assessment of  
349 Built Cultural Heritage) that has received funding from the European Research Council (ERC) under the  
350 European Union's Horizon 2020 research and innovation programme (Grant agreement No. 833123), as an  
351 Advanced Grant. In addition, the authors want to acknowledge the French Ministry of Education and Research  
352 for their financial support through a PhD grant attributed to the first author. The opinions and conclusions  
353 presented in this paper are those of the authors and do not necessarily reflect the views of the sponsoring  
354 organisations.

## 355 Competing interest

356 The authors declare there are no competing interests.

## 357 Authors' contribution

358 NS: Investigation, Formal Analysis, Visualisation, Writing – original draft; CM: Methodology, Resources,  
359 Investigation; EV: Funding acquisition, Writing – original draft, Methodology, Supervision; SF: Resources,  
360 Writing – review & editing, Methodology; PBL: Supervision, Funding acquisition, Writing – review & editing.

## 361 Data availability

362 The data arising from the analytical simulations presented in the paper is not available publicly.

## 363 References

364 [1] B. Villemus, J.-C. Morel, and C. Boutin, 'Experimental assessment of dry stone retaining wall stability on  
365 a rigid foundation', *Engineering Structures*, vol. 29, no. 9, pp. 2124–2132, 2006, doi:  
366 10.1016/j.engstruct.2006.11.007.

- 367 [2] A.-S. Colas, J.-C. Morel, and D. Garnier, 'Full-scale field trials to assess dry-stone retaining wall stability',  
368 *Engineering Structures*, vol. 32, no. 5, pp. 1215–1222, 2010, doi: 10.1016/j.engstruct.2009.12.047.
- 369 [3] A.-S. Colas, J.-C. Morel, and D. Garnier, 'Assessing the two-dimensional behaviour of drystone retaining  
370 walls by full-scale experiments and yield design simulation', *Géotechnique*, vol. 63, no. 2, pp. 107–117, 2013,  
371 doi: 10.1680/geot.10.P.115.
- 372 [4] C. Mundell, P. McCombie, C. Bailey, A. Heath, and P. Walker, 'Limit-equilibrium assessment of drystone  
373 retaining structures', *Proceedings of the Institution of Civil Engineers (Geotechnical Engineering)*, vol. 162, no.  
374 4, pp. 203–212, 2009, doi: 10.1680/geng.2009.162.4.203.
- 375 [5] L. R. Alejano, M. Veiga, J. Taboada, and M. Díez-Farto, 'Stability of granite drystone masonry retaining  
376 walls: I. Analytical design', *Géotechnique*, vol. 62, no. 11, pp. 1013–1025, 2012, doi: 10.1680/geot.10.P.112.
- 377 [6] A.-S. Colas, J.-C. Morel, and D. Garnier, 'Yield design modelling of dry joint retaining structures',  
378 *Construction and Building Materials*, vol. 41, pp. 912–917, 2013, doi: 10.1016/j.conbuildmat.2012.07.019.
- 379 [7] B. Terrade, A.-S. Colas, and D. Garnier, 'Upper bound limit analysis of masonry retaining walls using PIV  
380 velocity fields', *Meccanica*, vol. 53, no. 7, pp. 1661–1672, 2018, doi: 10.1007/s11012-017-0673-6.
- 381 [8] R. M. Harkness, W. Powrie, X. Zhang, K. C. Brady, and M.P. O'Reilly, 'Numerical modelling of full-scale  
382 tests on drystone masonry retaining walls', *Géotechnique*, vol. 50, no. 2, pp. 165–179, 2000, doi:  
383 10.1680/geot.2000.50.2.165.
- 384 [9] W. Powrie, R. M. Harkness, X. Zhang, and D. I. Bush, 'Deformation and failure modes of drystone  
385 retaining walls', *Géotechnique*, vol. 52, no. 6, pp. 435–446, 2002, doi: 10.1680/geot.2002.52.6.435.

- 386 [10] M. Claxton, R. A. Hart, P. F. McCombie, and P. J. Walker, 'Rigid block distinct-element modelling of dry-  
387 stone retaining walls in plane strain', *ASCE Journal of Geotechnical and Geoenvironmental Engineering*, vol. 131,  
388 no. 3, pp. 381–389, 2005, doi: 10.1061/(ASCE)1090-0241(2005)131:3(381).
- 389 [11] P. Walker, P. McCombie, and M. Claxton, 'Plane strain numerical model for drystone retaining walls',  
390 *Proceedings of the Institution of Civil Engineers - Geotechnical Engineering*, vol. 160, no. 2, pp. 97–103, 2007,  
391 doi: 10.1680/geng.2007.160.2.97.
- 392 [12] L. R. Alejano, M. Veiga, I. Gómez-Márquez, and J. Taboada, 'Stability of granite drystone masonry  
393 retaining walls: II. Relevant parameters and analytical and numerical studies of real walls', *Géotechnique*, vol.  
394 62, no. 11, pp. 1027–1040, 2012, doi: 10.1680/geot.10.P.113.
- 395 [13] J. J. Oetomo, E. Vincens, F. Dedecker, and J.-C. Morel, 'Modeling the 2D behavior of dry-stone retaining  
396 walls by a fully discrete element method', *International Journal for Numerical and Analytical Methods in  
397 Geomechanics*, vol. 40, no. 7, pp. 1099–1120, 2016, doi: 10.1002/nag.2480.
- 398 [14] Z. Li, Y. Zhou, and Y. Guo, 'Upper-Bound Analysis for Stone Retaining Wall Slope Based on Mixed  
399 Numerical Discretization', *International Journal of Geomechanics*, vol. 18, no. 10, pp. 1–14, 2018, doi:  
400 10.1061/(ASCE)GM.1943-5622.0001247.
- 401 [15] B. Pulatsu, S. Kim, E. Erdogmus, and P. B. Lourenço, 'Advanced analysis of masonry retaining walls using  
402 mixed discrete–continuum approach', *Proceedings of the Institution of Civil Engineers-Geotechnical  
403 Engineering*, pp. 1–13, 2020, doi: 10.1680/jgeen.19.00225.
- 404 [16] C. Mundell, P. McCombie, A. Heath, and J. Harkness, 'Behaviour of drystone retaining structures',  
405 *Proceedings of the Institution of Civil Engineers (Structures and Building)*, vol. 163, no. 1, pp. 3–12, 2010, doi:  
406 10.1680/stbu.2009.163.1.3.

- 407 [17] H. H. Le, D. Garnier, A.-S. Colas, B. Terrade, and J.-C. Morel, '3D homogenised strength criterion for  
408 masonry: Application to drystone retaining walls', *Journal of the Mechanics and Physics of Solids*, vol. 95, pp.  
409 239–253, 2016, doi: 10.1016/j.jmps.2016.05.021.
- 410 [18] H. H. Le, J.-C. Morel, A.-S. Colas, B. Terrade, and D. Garnier, 'Assessing the Three-Dimensional Behaviour  
411 of Dry Stone Retaining Walls by Full-Scale Experiments', *International Journal of Architectural Heritage*, vol. 14,  
412 no. 9, pp. 1373–1383, 2020, doi: 10.1080/15583058.2019.1607627.
- 413 [19] J.-C. Quezada, E. Vincens, R. Mouterde, and J.-C. Morel, '3D failure of a scale-down dry stone retaining  
414 wall : a DEM modelling', *Engineering Structures*, vol. 117, pp. 506–517, 2016, doi:  
415 10.1016/j.engstruct.2016.03.020.
- 416 [20] CAPEB, ABPS, Murailleurs de Provence, CBPS, CMA84, and ENTPE, *Pierres sèches : guide de bonnes  
417 pratiques de construction de murs de soutènement*. ENTPE, 2008.
- 418 [21] ENTPE, Artisans Bâisseurs en Pierre Sèche (ABPS), Ecole des Ponts ParisTech, IFSTTAR, and Fédération  
419 Française du Bâtiment (FFB), *Technique de construction des murs en pierre sèche : Règles professionnelles*.  
420 ENTPE, Artisans Bâisseurs en Pierre Sèche (ABPS), 2017.
- 421 [22] AFPS, *Recommandations AFPS 90*. Presses des Ponts et Chaussées Paris, 1990.
- 422 [23] H. H. Le, 'Stabilité des murs de soutènement routiers en pierre sèche : Modélisation 3D par le calcul à  
423 la rupture et expérimentation échelle 1', PhD Thesis, Ecole Nationale des Travaux Publics de l'Etat (ENTPE),  
424 2013.
- 425 [24] AFNOR, *NF EN 1997-1:2005 (Eurocode 7) : Geotechnical design - Part 1: General rules*, vol. 7, 8 vols.  
426 2005.



- 427 [25] AFNOR, *NF P 94-281 : Justification des ouvrages géotechniques - Normes d'application nationale de*  
428 *l'Eurocode 7 - Ouvrages de soutènement - Murs*. 2014.
- 429 [26] AFNOR, *NF P 94-261 : Justification des ouvrages géotechniques - Normes d'application nationale de*  
430 *l'Eurocode 7 - Fondations superficielles*. 2014.
- 431 [27] N. Savalle, E. Vincens, and S. Hans, 'Pseudo-static scaled-down experiments on dry stone retaining walls:  
432 Preliminary implications for the seismic design', *Engineering Structures*, vol. 171, pp. 336–347, Sep. 2018, doi:  
433 10.1016/j.engstruct.2018.05.080.
- 434 [28] AFNOR, *NF EN 1998-5:2005 (Eurocode 8) : Design of structures for earthquake resistance - Part 5:*  
435 *Foundations, retaining structures and geotechnical aspects*, vol. 8, 8 vols. 2005.
- 436 [29] AFNOR, *NF EN 1998-1:2005 (Eurocode 8) : Design of structures for earthquake resistance - Part 1:*  
437 *General rules, seismic actions and rules for buildings*, vol. 8, 8 vols. 2005.
- 438 [30] B. Villemus, 'Etude des Murs de Soutènement en Maçonnerie de Pierre Sèches', PhD Thesis, Ecole  
439 Nationale des Travaux Publics de l'Etat (ENTPE), 2004.
- 440 [31] C. A. Coulomb, *Essai sur une application des regles des maximis et minimis a quelques problemes de*  
441 *statique relatifs a l'architecture*, vol. 7. 1773.
- 442 [32] S. Okabe, 'General theory on earth pressure and seismic stability of retaining wall and dam', *Proc. Civil*  
443 *Engrg. Soc., Japan*, vol. 10, no. 6, pp. 1277–1323, 1924.
- 444 [33] N. Mononobe and H. Matsuo, 'On Determination of Earth Pressures during Earthquakes', in *World*  
445 *Engineering Conference*, 1929, vol. 9, pp. 177–185.
- 446 [34] N. Savalle, E. Vincens, and P. B. Lourenço, 'Pseudo-static analytical model for the static and seismic  
447 stability of dry stone retaining walls', Lisbon, Portugal, 2022. doi: 10.11159/icgre22.138.

- 448 [35] I. Ishibashi and Y.-S. FANG, 'Dynamic earth pressures with different wall movement modes', *Soils and*  
449 *Foundations*, vol. 27, no. 4, pp. 11–22, 1987.
- 450 [36] M. Ichihara and H. Matsuzawa, 'Earth pressure during earthquake', *Soils and Foundations*, vol. 13, no.  
451 4, pp. 75–86, 1973.
- 452 [37] N. Savalle, É. Vincens, and S. Hans, 'Experimental and numerical studies on scaled-down dry-joint  
453 retaining walls: Pseudo-static approach to quantify the resistance of a dry-joint brick retaining wall', *Bulletin of*  
454 *Earthquake Engineering*, vol. 18, pp. 581–606, Jan. 2020, doi: 10.1007/s10518-019-00670-9.
- 455 [38] A.-S. Colas, J.-C. Morel, and D. Garnier, 'Yield design of dry-stone masonry retaining structures -  
456 Comparisons with analytical, numerical, and experimental data', *International Journal for Numerical and*  
457 *Analytical Methods in Geomechanics*, vol. 32, no. 14, pp. 1817–1832, 2008, doi: 10.1002/nag.697.
- 458 [39] A.-S. Colas, 'Mécanique des murs de soutènement en pierre sèche : Modélisation par le calcul à la  
459 rupture et expérimentation échelle 1', PhD Thesis, Ecole Nationale des Travaux Publics de l'Etat (ENTPE), 2009.
- 460 [40] N. Savalle, 'Comportement sismique des murs de soutènement de talus en pierre sèche', PhD Thesis,  
461 Lyon, 2019. [Online]. Available: 10.5281/zenodo.4288880
- 462 [41] J. Wang and I. Thusyanthan, 'Evaluating foundation design concepts of Eurocode 7 & 8', 2008.
- 463 [42] A. Pecker and M. Pender, 'Earthquake resistant design of foundations: new construction', 2000.
- 464 [43] J. Koseki, R. J. Bathurst, E. Guler, J. Kuwano, and M. Maugeri, 'Seismic stability of reinforced soil walls',  
465 in *Proc. of 8th International Conference on Geosynthetics*, 2006, vol. 1, pp. 51–77.
- 466 [44] M. N. Fardis, *Seismic design, assessment and retrofitting of concrete buildings: based on EN-Eurocode 8*,  
467 vol. 8. Springer Science & Business Media, 2009.

- 468 [45] N. Savalle, J. Blanc-Gonnet, E. Vincens, and S. Hans, 'Dynamic behaviour of drystone retaining walls:  
469 shaking table scaled-down tests', *European Journal of Environmental and Civil Engineering*, vol. 26, no. 10, pp.  
470 4527–4547, 2022.
- 471 [46] N. Savalle, E. Vincens, S. Hans, and P. B. Lourenco, 'Dynamic Numerical Simulations of Dry-Stone  
472 Retaining Walls: Identification of the Seismic Behaviour Factor', *Geosciences*, vol. 12, no. 6, p. 252, 2022, doi:  
473 10.3390/geosciences12060252.
- 474 [47] K. C. Brady and J. Kavanagh, *Analysis of the stability of masonry-faced earth retaining walls*. Transport  
475 Research Laboratory Crowthorne, 2002.
- 476 [48] A.-S. Colas, J.-C. Morel, and D. Garnier, '2D modelling of a dry joint masonry wall retaining a pulverulent  
477 backfill', *International Journal for Numerical and Analytical Methods in Geomechanics*, vol. 34, no. 12, pp. 1237–  
478 1249, 2010, doi: 10.1002/nag.855.
- 479 [49] D. Giardini, J. Wössner, and L. Danciu, 'Mapping Europe's seismic hazard', *Eos, Transactions American*  
480 *Geophysical Union*, vol. 95, no. 29, pp. 261–262, 2014, doi: 10.1002/2014EO290001.

481